The Journal of Nutrition
Nutrition and Disease

High-Refined–Carbohydrate and High-Fat Diets Induce Comparable Hepatic Tumorigenesis in Male Mice[1–3]

Blanche C. Ip,[4,6] Chun Liu,[4] Donald E. Smith,[5] Lynne M. Ausman,[4,6] and Xiang-Dong Wang[4,6]*

[4]Nutrition and Cancer Biology Laboratory and [5]Comparative Biology Unit, Jean Mayer USDA Human Nutrition Research Center on Aging, and [6]Friedman School of Nutrition Science and Policy, Tufts University, Boston, MA

Abstract

Previous studies demonstrated that diet-induced obese mice fed a semi-purified high-fat diet (HFD) had greater liver tumorigenesis than mice fed a non-semi–purified diet. Because ingredients present in standard unpurified diets may elicit potential chemopreventive properties that are not present in semi-purified diets, the present study evaluated hepatic tumorigenic effects of dietary fat by replacing it with refined carbohydrates [digestible saccharides; high-carbohydrate diet (HCD)] in a semi-purified diet without altering other components. Two-wk-old *C57Bl/6J* male mice were randomly injected i.p. with either the liver-specific carcinogen diethylnitrosamine (25 mg/kg body weight) to induce liver cancer or saline as the nontumor control. At age 6 wk, mice with or without cancer initiation were further randomly assigned to an HFD (26% and 60% energy from carbohydrates and fat, respectively) or an HCD (66% and 12% energy from carbohydrates and fat, respectively) and consumed food ad libitum for 24 wk. Results showed that HCD-fed mice had a comparable degree of hepatic tumorigenesis (tumor number and volume) as HFD-fed mice, despite having significantly reduced body weights. HCD feeding induced greater hepatic endoplasmic reticulum (ER) stress-mediated protein kinase RNA-activated–like kinase (PERK) activation and oncogenic interleukin-6/signal transducer and activator of transcription 3 signaling than HFD feeding. HCD-stimulated PERK signaling was associated with elevated expression of prosurvival markers in tumors, including induced protein kinase B activation, increased extracellular signal-regulated kinases 1/2 phosphorylation, and elevated cyclin D1 protein expression. However, HCD-mediated PERK activation in tumors was also positively associated with markers of proapoptosis, which included elevated CCAAT/enhancer-binding protein homology protein expression and increased cleaved caspase-3. HCD-fed mice had greater severity in hepatic steatosis than HFD-fed mice. HCD-induced steatosis exacerbation was associated with increased expression in hepatic de novo lipogenic markers that can promote ER stress. Together, these data indicated that chronic HCD consumption by mice can produce comparable severity of hepatic tumorigenesis as HFD consumption, potentially through upregulating PERK-mediated ER stress. J. Nutr. 144: 647–653, 2014.

Introduction

Liver cancer is the third leading cause of cancer-related deaths worldwide (1), and hepatocellular carcinoma (HCC)[7] is the most frequent and aggressive type of primary liver tumor (1). The morbidity and mortality from HCC are parallel to the increasing prevalence of non-alcoholic fatty liver disease (NAFLD) (2), which is a non-alcohol–related form of steatosis that is present in 75–100% of overweight and obese adults and children (2). The molecular mechanisms involved in NAFLD-associated HCC development are thought to include elevated systemic inflammation, dysregulated lipid metabolism, and activated mitogen signaling related to insulin resistance (3–5).

[1] Supported by NIH grant CA104932, USDA/Agricultural Research Service grant 1950-51000-074S, and NIH/National Heart, Lung, and Blood Institute grants 5T32HL069772-10 and 2T32HL069772-11A1. Any opinions, findings, conclusions, and recommendations expressed in this publication are those of the authors and do not necessarily reflect the views of the sponsors.
[2] Author disclosures: B. C. Ip, C. Liu, D. E. Smith, L. M. Ausman, and X.-D. Wang, no conflicts of interest.
[3] Supplemental Figure 1 and Supplemental Tables 1 and 2 are available from the "Online Supporting Material" link in the online posting of the article and from the same link in the online table of contents at http://jn.nutrition.org.
* To whom correspondence should be addressed. E-mail: xiang-dong.wang@tufts.edu.

[7] Abbreviations used: ACC, acetyl-CoA carboxylase; Akt, protein kinase B; CHOP, CCAAT/enhancer-binding protein homology protein; cIAP1, cellular inhibitor of apoptosis protein; DEN, diethylnitrosamine; DIO, diet-induced obesity; DNL, de novo lipogenesis; eIF2α, eukaryotic initiation factor 2α; ER, endoplasmic reticulum; ER^{UPR}, endoplasmic reticulum-stress-mediated unfolded protein response; Erk, MAPK–extracellular signal-regulated kinase; HCC, hepatocellular carcinoma; HCD, high-carbohydrate diet or diet high in refined carbohydrates (digestible saccharides); HFD, high-fat diet; IκB, NF-κB-inhibitory protein inhibitory κB; NAFLD, non-alcoholic fatty liver disease; PERK, protein kinase RNA-activated–like kinase; RPS6, ribosomal protein S6; SCD1, stearoyl-CoA desaturase 1; STAT3, signal transducer and activator of transcription 3.

Manuscript received December 12, 2013. Initial review completed January 30, 2014. Revision accepted February 28, 2014.
First published online March 19, 2014; doi:10.3945/jn.113.189613.

Previous studies demonstrated that mice with diet-induced obesity (DIO) from consuming a semi-purified high-fat diet (HFD) (60% of energy derived from fat) promoted greater liver tumorigenesis than that in mice fed a standard unpurified diet (4,6). The mechanisms by which DIO promoted tumorigenesis were related to systemic elevations of free FAs and the increased presence of the proinflammatory cytokines tumor necrosis factor-α and interleukin-6 (IL-6) (4,6). DIO promoted these proinflammatory responses by inducing the nuclear factor-κB (NF-κB), MAPK, and IL-6/signal transducer and activator of transcription 3 (STAT3) signaling pathways (3–6). STAT3-activated tumors in humans have been observed to be more aggressive than tumors without STAT3 activation (3–6). Because unpurified diets (12% of energy from fat) contain other ingredients (e.g., phytonutrients and fiber) with potential chemopreventative properties that are not present in semi-purified diets, reports comparing outcomes between HFD-fed and unpurified diet–fed mice may be not appropriate to evaluate the tumorigenic effects of dietary fat alone.

Epidemiologic studies suggested that a diet high in refined carbohydrates (HCD) (50–65% of energy from carbohydrates, high glycemic index, and low in fiber) could promote NAFLD progression (7–9) and was associated with increased HCC risk (10). These observational data have been consistent with comparable experimental reports. Mice fed a high glycemic index diet for 24 wk had greater hepatic TGs and adiposity than mice fed a low glycemic index diet (11). HCD has been shown to induce hepatic de novo lipogenesis (DNL) and increased synthesis of lipogenic enzymes (12,13). As a result, the demand for endoplasmic reticulum (ER)–assisted folding becomes elevated (14,15), leading to the induction of an ER stress-mediated unfolded protein response (ER^{UPR}) (14,15). Metabolic excess-induced ER^{UPR} activation has been associated with liver cancer development (16). Furthermore, ER stress could also induce fibrogenic activity of hepatic stellate cells (17). Hepatic fibrosis can promote the development of liver cirrhosis (5), which is a significant risk factor for HCC development (5). This evidence begs the question as to whether HFD would indeed promote greater hepatic tumorigenesis (when compared with HCD) and whether the remaining compositions of the diets were similar.

The present study investigated the liver tumorigenic effects of dietary fat in a carcinogen-initiated HCC mouse model by replacing dietary fat with refined carbohydrates (digestible saccharides) without altering other dietary components. In addition, we explored potential mechanisms by which HCD exhibited its hepatic tumorigenic effects by inducing ER^{UPR}.

Materials and Methods

Study design. The experimental protocol (**Supplemental Fig. 1***A*) was adapted from a well-established animal model for studying HCC pathogenesis (4,18) and approved by the Institutional Animal Care and Use Committee at the Jean Mayer USDA Human Nutrition Research Center on Aging at Tufts University. Pregnant female *C57Bl/6J* mice were purchased from The Jackson Laboratory to generate male mice for this study. Mice consumed water and food ad libitum and were maintained in an environmentally controlled (12-h light/dark cycle, temperature and humidity controlled) animal room throughout the study. Two-wk-old mice were randomly injected i.p. with either saline (−DEN arm) or with the liver-specific carcinogen diethylnitrosamine (DEN; Sigma-Aldrich) (+DEN arm) at a dose of 25 mg/kg body weight as described previously (4,18). At age 6 wk, mice under both the −DEN and +DEN arms were randomly assigned to either a HFD (HFD − DEN or HFD + DEN; F3283; Bio-Serv) (composition in **Supplemental Table 1**) or HCD (HCD − DEN or HCD + DEN; F6395; Bio-Serv) (Supplemental Table 1). All mice were killed without being food deprived at age 30 wk by terminal exsanguination under deep isoflurane (Isothesia; Butler Schein) anesthesia.

Quantification of liver tumors. After the mice were killed, whole livers were removed from study mice and processed for biochemical and histologic analyses as described previously (18). Primary outcomes, including liver tumor multiplicity, were evaluated by two investigators unaware of treatments, as described previously (18).

Histopathologic evaluation. Sections (*5* μm) of formalin-fixed, paraffin-embedded liver tissue were subjected to hematoxylin and eosin staining and histopathologic examination by two independent investigators unaware of the treatment groups as described previously (18).

RNA extraction and qRT-PCR. Total RNA extraction from frozen liver tissue and subsequent qRT-PCR were performed as described previously (18). Primer sequences are listed in **Supplemental Table 2**.

Protein isolation and Western blotting. Protein isolation from frozen liver tissue and subsequent Western blotting analysis of specific proteins were executed as described previously (18). The following antibodies were used for Western blotting: *1*) acetyl-CoA carboxylase (ACC); *2*) protein kinase B (Akt); *3*) eukaryotic initiation factor 2α (eIF2α); *4*) MAPK–extracellular signal-regulated kinases 1/2 (Erk1/2); *5*) protein kinase RNA-activated–like kinase (PERK); *6*) phosphorylated Akt (Ser473); *7*) phosphorylated eIF2α (Ser51); *8*) phosphorylated p44/42 MAPK–Erk1/2 (Thr202/Tyr204); *9*) phosphorylated PERK (Thr980); *10*) phosphorylated STAT3 (Tyr705); *11*) stearoyl-CoA desaturase 1 (SCD1); *12*) STAT3 (Cell Signaling Technology); *13*) IL-6 (R&D Systems); *14*) CCAAT/enhancer-binding protein homology protein [CHOP (or GADD153)]; and *15*) cyclin D1 (Santa Cruz Biotechnology). Proteins were detected by a horseradish peroxidase–conjugated secondary antibody (Bio-Rad). The specific bands were visualized by a SuperSignal West Pico Chemiluminescent Substrate Kit (Pierce) according to the instructions of the manufacturer. Anti-actin antibody (Sigma-Aldrich) was used to detect β-actin used for the equal loading of some proteins. The intensities of bands were quantified by using GS-710 Calibrated Imaging Densitometer (Bio-Rad).

Statistical analysis. SAS 9.3 software was used to perform the statistical analyses. Student's *t* test and nonparametric Wilcoxon's signed rank tests were used to examine the differences in primary outcome measurements for the following comparisons: *1*) HFD − DEN and HCD − DEN; *2*) HFD + DEN (nontumor) and HCD + DEN (nontumor); and *3*) HFD + DEN (tumor) and HCD + DEN (tumor). Spearman's rank correlation was used to perform nonparametric measures of statistical dependence between two variables. *P* value was set at 0.05 for comparisons to reach statistical significance.

Results

HCD- or HFD-fed mice had the same degree of DEN-initiated hepatic tumorigenesis. No liver tumors were detected in uninitiated HFD-fed and HCD-fed mice (HFD − DEN and HCD − DEN; **Table 1**). All DEN-initiated mice (HFD + DEN and HCD + DEN) developed multiple surface liver tumors (Supplemental Fig. 1*Bi*, *Bii*; Table 1), similar to those described in previously published studies (4,18). Hematoxylin and eosin staining of *C57Bl/6J* liver tissues showed hepatic adenoma and HCC development (Supplemental Fig. 1*Biii*, *Biv*), with inflammatory cell infiltration within both tumor and nontumor regions (Supplemental Fig. 1*Bv*, *Bvi*). Hepatic surface tumor multiplicity and volume were not statistically different between the HFD + DEN and HCD + DEN groups (Table 1). Final body weights of HFD-fed mice were comparable with the *C57Bl/6J* DIO phenotype as described previously (4,19). HCD-fed mice weighed ~10 g less than HFD-fed mice within each DEN arm of this study (Table 1)

TABLE 1 Liver tumor outcomes, body and liver weights, hepatic steatosis, and inflammation in *C57BL/6J* male mice that were or were not treated with DEN to initiate liver cancer, fed either an HFD or HCD for 24 wk[1]

	Study group			
	HFD − DEN	HCD − DEN	HFD + DEN	HCD + DEN
Mice, *n*	7	8	27	26
Mortality, *n*	1	0	3	1
Liver tumor outcomes				
Incidence, %	0	0	100	100
Multiplicity, *n*	0	0	14.6 ± 1.9	10.9 ± 1.2
Volume, mm^3	0	0	306 ± 113	338 ± 154
Final body weights, *g*	52.9 ± 1.4	44.3 ± 1.4*	50.9 ± 0.6	41.2 ± 0.6*
Liver weights, *g*	2.6 ± 0.1	2.5 ± 0.1	2.4 ± 0.1	2.5 ± 0.2
Liver/body weight, %	4.9 ± 0.1	5.8 ± 0.2*	4.2 ± 0.2	6.2 ± 0.5*
Hepatic steatosis score[2]	2 (1–2)	3 (2–4)*	2 (1–3)	2 (0–3)*
Liver inflammatory foci, n/cm^2	0.0 ± 0.0	0.6 ± 0.4	1.7 ± 0.5	1.4 ± 0.3

[1] Values are means ± SEMs or medians (ranges) unless otherwise noted. *Different from the corresponding HFD, $P < 0.05$. DEN, diethylnitrosamine; HCD, diet high in refined carbohydrates; HFD, high-fat diet.
[2] The means for the hepatic steatosis were 1.83 and 2.15 for HFD + DEN and HCD + DEN, respectively. Wilcoxon's signed-rank test was used to examine the difference between steatosis medians.

but were ~10 g heavier than unpurified diet–fed mice (~32 g at age 30 wk) in previously published studies (4,19). All groups of mice in the current study had similar degrees of mortality (Table 1).

HCD feeding induced more severe hepatic steatosis and greater DNL enzyme expression than HFD feeding. HCD-fed mice had more severe hepatic steatosis than HFD-fed mice (Supplemental Fig. 1*Bvii*, *Bviii*; Table 1). HCD feeding induced greater protein expression of DNL enzymes in liver and liver tumor tissue than HFD feeding, including ACC [by 122% in HCD − DEN, 294% in HCD + DEN (nontumor), and 316% in HCD + DEN (tumor)] (**Fig. 1***A*) and SCD1 [by 659% in HCD − DEN, 243% in HCD + DEN (nontumor), and 116% in HCD + DEN (tumor)] (Fig. 1*B*). This HCD-associated DNL enzyme protein induction in liver tissue accompanied elevated gene expression of *Acc* [by 249% in HCD − DEN and 186% in HCD + DEN (nontumor)] (Fig. 1*C*), *Scd1* [by 498% in HCD − DEN and 348% in HCD + DEN (nontumor)] (Fig. 1*C*), and FA synthase [by 298% in HCD − DEN and 219% in HCD + DEN (nontumor)] (Fig. 1*C*), thus implying an HCD-induced transcriptional regulation of these DNL enzymes. This phenomenon was not observed in liver tumor tissue (Fig. 1*C*).

HCD-fed mice had greater ER^{UPR}-associated PERK/eIF2α signaling induction than HFD-fed mice. Replacing dietary fats with refined carbohydrates induced activation of PERK by phosphorylation [by 106% in HCD − DEN, 96% in HCD + DEN (nontumor), and 89% in HCD + DEN (tumor)] (**Fig. 2***A*) in liver and liver tumor tissue in each DEN arm. This HCD-mediated PERK activation was associated with the increased phosphorylation of the PERK-downstream signaling molecule eIF2α [by 10-fold in HCD − DEN, 75% in HCD + DEN (nontumor), and 63% in HCD + DEN (tumor)] (Fig. 2*B*). Hepatic PERK activation in the +DEN arm was correlated with eIF2α phosphorylation in liver and liver tumor tissue ($R^2 = 0.49$, $P = 0.001$; and $R^2 = 0.50$, $P = 0.007$, respectively). PERK and eIF2α phosphorylation in the +DEN arm also correlated with ACC (PERK: $R^2 = 0.37$, $P = 0.019$; eIF2: $R^2 = 0.36$, $P = 0.018$) and SCD1 (PERK: $R^2 = 0.30$, $P = 0.049$; eIF2α: $R^2 = 0.43$, $P = 0.003$) protein expression in liver tissue. There was a suggestive correlation between eIF2α phosphorylation and SCD1 ($R^2 = 0.35$, $P = 0.08$) in liver tumors. HFD- and HCD-fed mice shared similar ER^{UPR}-associated inositol requiring enzyme 1α-mediated X-box binding protein 1 gene expression and splicing in liver tissue (data not shown).

HCD feeding induced greater proinflammatory signaling activation than HFD-fed mice. HCD-mediated PERK/eIF2α activation in the +DEN arm was associated with induced IL-6 protein expression (by 79%) (Fig. 2*C*) and IL-6-dependent oncogenic STAT3 phosphorylation (by 80%) (Fig. 2*D*) in liver tissue. IL-6 expression was correlated with the phosphorylation of PERK ($R^2 = 0.52$, $P < 0.001$) and eIF2α ($R^2 = 0.55$, $P < 0.001$), as well as with ACC ($R^2 = 0.48$, $P < 0.001$) and SCD1 ($R^2 = 0.29$, $P = 0.08$) protein expression. We observed no differences in the protein expression of NF-κB-inhibitory protein inhibitory κB (IκB) (data not shown).

HCD feeding induced Akt and MAPK/Erk signaling in liver tumors. Replacing dietary fat with refined carbohydrates induced Akt activation by phosphorylation (by 382%) (**Fig. 3***A*) in liver tumors. HCD-mediated Akt activation was associated with the activation of Erk1/2 by phosphorylation (by 144%) (Fig. 3*B*), cyclin D1 protein expression (by 104%) (Fig. 3*C*), and with increased Erk-mediated downstream gene target cellular inhibitor of apoptosis protein (*cIAP1*; by 20%; $P = 0.08$) (Fig. 3*D*). We observed correlations between Akt activation and Erk1/2 phosphorylation ($R^2 = 0.49$, $P = 0.006$), eIF2α phosphorylation ($R^2 = 0.38$, $P = 0.045$), CHOP ($R^2 = 0.40$, $P = 0.030$), and SCD1 ($R^2 = 0.47$, $P = 0.019$) protein expression. Erk1/2 phosphorylation was correlated with eIF2α phosphorylation ($R^2 = 0.55$, $P = 0.002$) and SCD1 protein expression ($R^2 = 0.55$, $P = 0.004$). There was no difference in ribosomal protein S6 (RPS6) phosphorylation between HFD and HCD tumors (data not shown).

HFD feeding reduced expression of proapoptotic markers in liver tumors. HCD feeding induced greater proapoptotic CHOP protein expression than HFD feeding in the liver and liver tumor tissue [by 316% in HCD − DEN, 105% in HCD + DEN (nontumor), and 68% in HCD + DEN (tumor)] (Fig. 3*E*). HCD-associated CHOP protein upregulation in liver tumors accompanied the induction of cleaved caspase-3 (by 485%) (Fig. 3*F*),

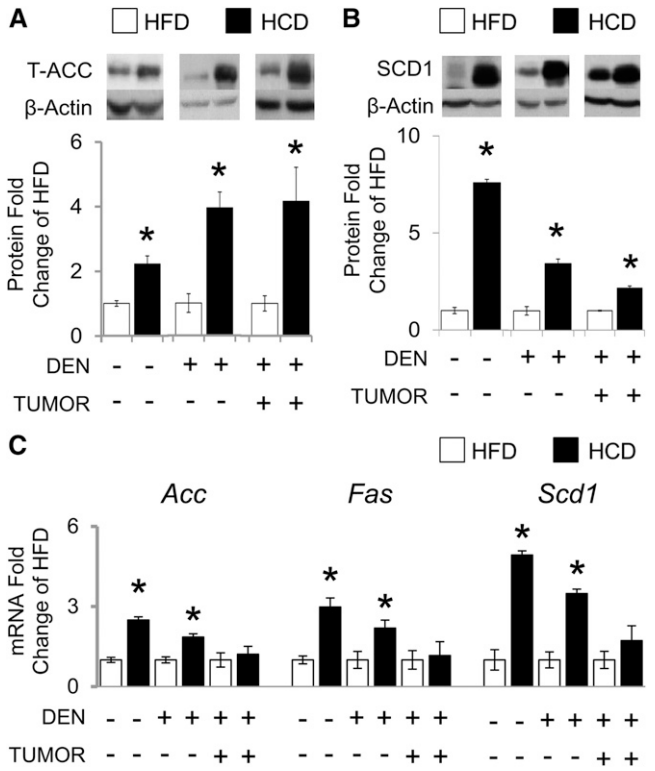

FIGURE 1 Hepatic DNL biomarkers in *C57BL/6J* male mice that were or were not treated with DEN to initiate liver cancer, fed either an HFD or HCD for 24 wk. Graphical representation of fold changes: *A*) ACC protein; *B*) SCD1 protein; *C*) *Acc* mRNA, *Fas* mRNA, and *Scd1* mRNA. Representative Western blots with 1 sample per group are shown. −DEN arm, n = 6–7 per group; +DEN arm (nontumor), n = 22–26 per group; +DEN arm (tumor), n = 12–16 per group. Fold changes normalized to HFD − DEN, HFD + DEN (nontumor), or HFD + DEN (tumor). Values are means ± SEMs. *Different from the corresponding HFD, $P < 0.05$. *Acc*, acetyl-CoA carboxylase; DEN, diethylnitrosamine; DNL, de novo lipogenesis; *Fas*, FA synthase; HCD, diet high in refined carbohydrates; HFD, high-fat diet; *Scd1*, stearoyl-CoA desaturase 1; T-, total.

suggesting cancer cell apoptosis. CHOP protein expression correlated with SCD1 protein expression ($R^2 = 0.39$, $P = 0.007$) in the liver tissue and had a suggestive correlation with PERK phosphorylation ($R^2 = 0.33$, $P = 0.09$) in liver tumors.

Discussion

The present study provided a novel observation that HCD and HFD feeding had similar effects on DEN-induced liver tumorigenesis in male mice, suggesting that dietary fat did not have greater tumorigenic effects on the liver than dietary refined carbohydrates. This outcome occurred despite the fact that HCD-fed mice weighed significantly less than HFD-fed mice, presumably because of the differential energy densities of the diets. Therefore, HCD feeding may use alternative pathways to promote liver tumorigenesis than those that are obesity- and/or weight-dependent.

ER^{UPR} plays an important role in NAFLD development and progression (16,20), and we investigated whether ER^{UPR} could be induced with HCD or HFD feeding. ER^{UPR} is characterized by the activation of three distinct signal transduction pathways originating from the ER membrane that are mediated by the inositol requiring enzyme 1α/X-box binding protein 1 system, PERK/eIF2α signaling, and the activation of transcription factor 6α (16,20). We observed that replacing dietary fat with refined carbohydrates significantly induced PERK/eIF2α signaling in both liver and liver tumor tissue. It has been reported that PERK/eIF2α activation was important for cancer cell survival (21,22). Genetic ablation of PERK or a knock-in mutation of the PERK phosphorylation site on eIF2α both significantly reduced the survival of transformed mouse embryo fibroblasts (22). Because others reported that tumors in PERK knockout mice grew much slower and exhibited a greater degree of apoptosis than in the respective wild-type mice (22), our results suggested that refined carbohydrates may promote liver tumorigenesis through eliciting PERK/eIF2α signaling. This notion is in support of observations that patients with NAFLD and non-alcoholic steatohepatitis had increased eIF2α phosphorylation and glucose-regulated protein 78/binding Ig protein expression (23), suggesting a positive association between ER^{UPR} and NAFLD progression.

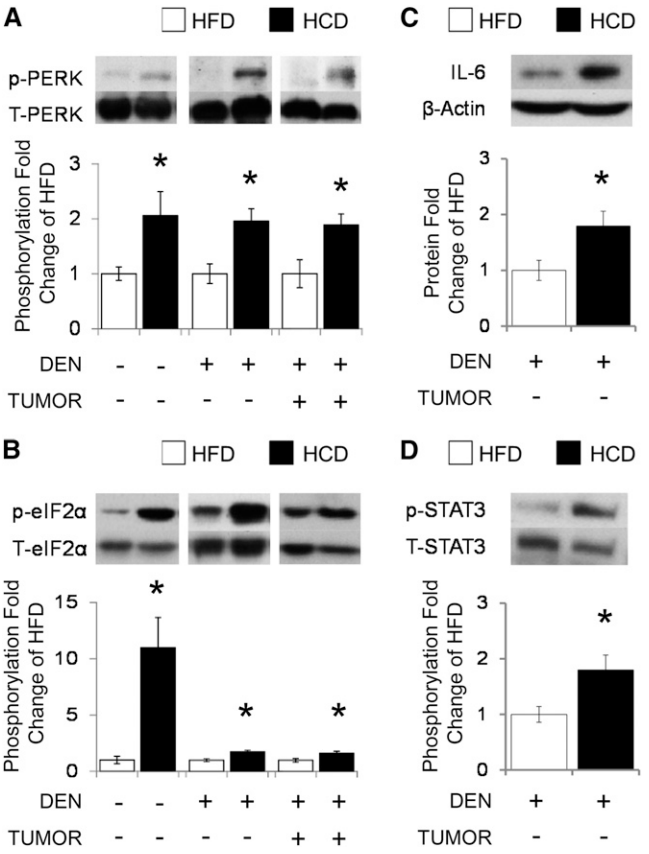

FIGURE 2 Hepatic PERK/eIF2α signaling and apoptotic markers in *C57BL/6J* male mice that were and were not treated with DEN to initiate liver cancer, fed either an HFD or HCD for 24 wk. Graphical representation of fold changes: *A*) PERK (Thr980) phosphorylation (total PERK as control); *B*) eIF2α (Ser51) phosphorylation (total eIF2α as control); *C*) IL-6 protein; *D*) STAT3 (Tyr705) phosphorylation (STAT3 as control). Representative Western blots with 1 sample per group are shown. −DEN arm, n = 6–7 per group; +DEN arm (nontumor), n = 22–26 per group; +DEN arm (tumor), n = 12–16 per group. Fold changes normalized to HFD − DEN, HFD + DEN (nontumor), or HFD + DEN (tumor). Values are means ± SEMs. *Different from the corresponding HFD, $P < 0.05$. DEN, diethylnitrosamine; eIF2α, eukaryotic initiation factor 2α; HCD, diet high in refined carbohydrates; HFD, high-fat diet; p-, phosphorylated; PERK, protein kinase RNA-activated-like kinase; STAT3, signal transducer and activator of transcription 3; T-, total.

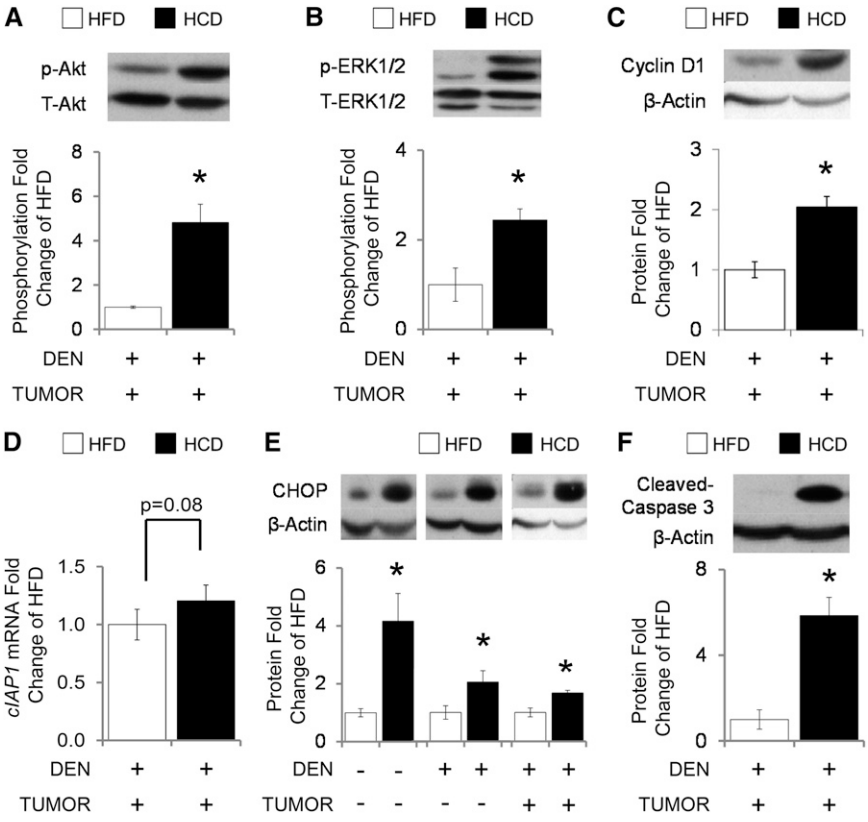

FIGURE 3 Liver tumor Akt, MAPK/Erk, and IL-6 signaling in *C57BL/6J* male mice fed either an HFD or HCD for 24 wk. Graphical representation of fold changes: *A*) Akt (Ser473) phosphorylation (total Akt as control); *B*) Erk1/2 (Thr202/Tyr204) phosphorylation (total Erk1/2 as control); *C*) cyclin D1; *D*) *cIAP1* mRNA; *E*) CHOP; *F*) cleaved caspase 3. Representative Western blots with 1 sample per group are shown. −DEN arm, n = 6–7 per group; +DEN arm (nontumor), n = 22–26 per group; +DEN arm (tumor), n = 12–16 per group. Fold changes normalized to HFD − DEN, HFD + DEN (nontumor), or HFD + DEN (tumor). Values are means ± SEMs. *Different from the corresponding HFD, $P < 0.05$. Akt, protein kinase B; CHOP, CCAAT/enhancer-binding protein homology protein; *cIAP1*, cellular inhibitor of apoptosis protein; DEN, diethylnitrosamine; Erk, MAPK–extracellular signal-regulated kinase; HCD, diet high in refined carbohydrates; HFD, high-fat diet; p-, phosphorylated; T-, total.

ER^{UPR} has been linked to major inflammatory signaling networks, including the NF-κB pathway and the NF-κB-inducible cytokine IL-6 expression (5,20). We observed that HCD-induced PERK/eIF2α signaling activation was associated with increased IL-6 protein expression and STAT3 phosphorylation. This phenomenon occurred in the absence of IκB modulation. It has been suggested that PERK/eIF2α-dependent NF-κB signaling promotion can be mediated through the transcriptional repression of IκB (24). PERK/eIF2α can also activate NF-κB signaling in a non-IκB degradation–dependent mechanism, involving the induced disassociation of IκBα from the NF-κB p65 subunit (25). Our results suggest that HCD feeding may have induced NF-κB activation in an IκB-independent manner.

Interestingly, HCD-induced PERK/eIF2α signaling activation in the current study was associated with elevated Akt-Erk1/2 signaling activation. This observation was accompanied with the HCD-promoted increase in cyclin D1 protein expression and a nonsignificant increase in the Erk-mediated downstream gene target, the anti-apoptotic *cIAP1*. The induction of the phosphatidylinositol 3-kinase–Akt pathway is important to facilitate cancer cell survival, which requires PERK/eIF2α signaling (26–28). The potential mechanisms for the PERK-induced prosurvival included the Akt-mediated activation of MAPK/Erk signaling (27), as well as the induction of cIAP1 and cIAP2 proteins (26,29). Akt activation in transformed cells of human liver tumors is a risk factor for early disease recurrence (30,31) and correlates with increased cell cycle promoter cyclin D1 expression (27,32).

Although our observation suggests that replacing dietary fat with refined carbohydrates may promote tumor growth through Akt–Erk signaling activation, both HCD-fed and HFD-fed mice had comparable tumor volume. PERK/eIF2α signaling activation can initiate the gene activation of transcription factor 4 translation, a transcription factor that induces the expression of the proapoptotic protein CHOP (16). In the present study, HCD-induced PERK/eIF2α signaling was associated with elevated CHOP protein expression in liver tumors. This evidence suggests that HCD-mediated PERK/eIF2α activation may promote tumor cell apoptosis, as indicated by the HCD-induced elevation in cleaved caspase 3. These proapoptotic properties of PERK/eIF2α activation may counteract the tumor-proliferating effects of Akt signaling in HCD-fed mice, providing a plausible explanation to why HCD-fed mice had similar hepatic tumorigenesis as HFD-fed mice.

Metabolic excess and/or obesity-related hepatic ER stress stemmed from accumulation of misfolded protein, a phenomenon that was partially due to increased synthesis of proteins involved in lipid metabolism (synthesis, oxidation, transport) (14,33,34). In the present study, HCD-fed mice had more severe hepatic steatosis than HFD-fed mice, regardless of liver tumor bearing. This HCD-induced elevated steatosis was associated with the significant upregulation of DNL genes and proteins, including ACC and SCD-1, as well as FA synthase gene expression. This evidence is consistent with previous in vivo studies and clinical observations that HCD-induced NAFLD was associated with elevated hepatic DNL (7–9). Donnelly et al. (35) observed that patients with NAFLD have elevated fasting DNL compared with healthy individuals. Altering dietary macronutrient contents can induce differential metabolic consequences in the liver (8,14,36). Excessive dietary carbohydrates induced glucose conversion to FA by DNL (8,36), whereas excessive dietary fat elevated hepatic lipid uptake without stimulating DNL (14,36). *C57BL/6J* mice fed an HFD for 500 d had significantly reduced mRNA expression of DNL genes compared with unpurified diet–fed mice, suggesting a potential negative feedback on lipogenesis by excessive dietary fat (6). In the current study, we observed that HCD-induced DNL was correlated with PERK/eIF2α signaling activation, providing evidence to support the notion that aberrant lipid metabolism, including elevated lipogenesis, was an important contributor to hepatic ER stress (20).

It is important to note that ER^{UPR} also has lipogenic capacity (15), whereas Akt signaling activation can induce lipogenesis in a mammalian target of rapamycin complex 1/RPS6-dependent manner (31). Therefore, we are unable to conclude whether HCD-induced DNL preceded the ER^{UPR}-associated PERK/eIF2α signaling. Interestingly, HCD feeding did not induce RPS6 phosphorylation in tumor regions. This observation provided some evidence to suggest that HCD feeding may promote hepatic steatosis in an Akt-independent manner. Additional investigations are required to determine whether HCD-promoted hepatic steatosis is independent of ER^{UPR}. We also acknowledge that the basal diet for this study lacked dietary fiber. Low dietary fiber is associated with increased prevalence for metabolic syndrome and HCC risk in humans (10). Diets rich in complex carbohydrates and fiber did not induce clinical DNL in humans, suggesting a potential interaction between digestibility/structure of carbohydrates and DNL (13).

Together, the present study proposed that chronic HCD feeding can promote comparable severity of hepatic tumorigenesis as for HFD feeding potentially through upregulating PERK-mediated ER stress.

Acknowledgments

The authors thank Drs. Alice H. Lichtenstein and Martin S. Obin for providing valuable comments on this manuscript. B.C.I. and X.-D.W. designed the research; B.C.I., C.L., D.E.S., and X.-D.W. conducted the research; B.C.I. analyzed the data; B.C.I., L.M.A., and X.-D.W. wrote the paper; and X.-D.W. had primary responsibility for final content. All authors read and approved the final manuscript.

Literature Cited

1. Jemal A, Bray F, Center MM, Ferlay J, Ward E, Forman D. Global cancer statistics. CA Cancer J Clin. 2011;61:69–90.
2. Baffy G, Brunt EM, Caldwell SH. Hepatocellular carcinoma in non-alcoholic fatty liver disease: an emerging menace. J Hepatol. 2012;56:1384–91.
3. Wang Y, Ausman LM, Greenberg AS, Russell RM, Wang XD. Nonalcoholic steatohepatitis induced by a high-fat diet promotes diethylnitrosamine-initiated early hepatocarcinogenesis in rats. Int J Cancer. 2009;124:540–6.
4. Park EJ, Lee JH, Yu GY, He G, Ali SR, Holzer RG, Osterreicher CH, Takahashi H, Karin M. Dietary and genetic obesity promote liver inflammation and tumorigenesis by enhancing IL-6 and TNF expression. Cell. 2010;140:197–208.
5. Sun B, Karin M. Obesity, inflammation, and liver cancer. J Hepatol. 2012;56:704–13.
6. Hill-Baskin AE, Markiewski MM, Buchner DA, Shao H, DeSantis D, Hsiao G, Subramaniam S, Berger NA, Croniger C, Lambris JD. Diet-induced hepatocellular carcinoma in genetically predisposed mice. Hum Mol Genet. 2009;18:2975–88.
7. Toshimitsu K, Matsuura B, Ohkubo I, Niiya T, Furukawa S, Hiasa Y, Kawamura M, Ebihara K, Onji M. Dietary habits and nutrient intake in non-alcoholic steatohepatitis. Nutrition. 2007;23:46–52.
8. Solga S, Alkhuraishe AR, Clark JM, Torbenson M, Greenwald A, Diehl AM, Magnuson T. Dietary composition and nonalcoholic fatty liver disease. Dig Dis Sci. 2004;49:1578–83.
9. Valtueña S, Pellegrini N, Ardigò D, Del Rio D, Numeroso F, Scazzina F, Monti L, Zavaroni I, Brighenti F. Dietary glycemic index and liver steatosis. Am J Clin Nutr. 2006;84:136–42.
10. Fedirko V, Lukanova A, Bamia C, Trichopolou A, Trepo E, Nöthlings U, Schlesinger S, Aleksandrova K, Boffetta P, Tjønneland A. Glycemic index, glycemic load, dietary carbohydrate, and dietary fiber intake and risk of liver and biliary tract cancers in Western Europeans. Ann Oncol. 2013;24:543–53.
11. Scribner KB, Pawlak DB, Ludwig DS. Hepatic steatosis and increased adiposity in mice consuming rapidly vs. slowly absorbed carbohydrate. Obesity (Silver Spring). 2007;15:2190–9.
12. Schwarz JM, Linfoot P, Dare D, Aghajanian K. Hepatic de novo lipogenesis in normoinsulinemic and hyperinsulinemic subjects consuming high-fat, low-carbohydrate and low-fat, high-carbohydrate isoenergetic diets. Am J Clin Nutr. 2003;77:43–50.
13. Hudgins LC, Hellerstein MK, Seidman CE, Neese RA, Tremaroli JD, Hirsch J. Relationship between carbohydrate-induced hypertriglyceridemia and fatty acid synthesis in lean and obese subjects. J Lipid Res. 2000;41:595–604.
14. Ren LP, Chan SMH, Zeng XY, Laybutt DR, Iseli TJ, Sun RQ, Kraegen EW, Cooney GJ, Turner N, Ye JM. Differing endoplasmic reticulum stress response to excess lipogenesis versus lipid oversupply in relation to hepatic steatosis and insulin resistance. PLoS One. 2012;7:e30816.
15. Lee A-H, Scapa EF, Cohen DE, Glimcher LH. Regulation of hepatic lipogenesis by the transcription factor XBP1. Science. 2008;320:1492–6.
16. Malhi H, Kaufman RJ. Endoplasmic reticulum stress in liver disease. J Hepatol. 2011;54:795–809.
17. Hernández-Gea V, Hilscher M, Rozenfeld R, Lim MP, Nieto N, Werner S, Devi LA, Friedman SL. Endoplasmic reticulum stress induces fibrogenic activity in hepatic stellate cells through autophagy. J Hepatol. 2013;59:98–104.
18. Ip BC, Hu KQ, Liu C, Smith DE, Obin MS, Ausman LM, Wang XD. Lycopene metabolite, apo-10′-lycopenoic acid, inhibits diethylnitrosamine-initiated, high fat diet-promoted hepatic inflammation and tumorigenesis in mice. Cancer Prev Res (Phila). 2013;6:1304–16.
19. The Jackson Laboratory. C57BL/6J diet-induced obesity (DIO) phenotype. 2014. Available from: http://jaxmice.jax.org/diomice/diomice-phenotypes.html.
20. Fu S, Watkins SM, Hotamisligil GS. The role of endoplasmic reticulum in hepatic lipid homeostasis and stress signaling. Cell Metab. 2012;15:623–34.
21. Koumenis C, Naczki C, Koritzinsky M, Rastani S, Diehl A, Sonenberg N, Koromilas A, Wouters BG. Regulation of protein synthesis by hypoxia via activation of the endoplasmic reticulum kinase PERK and phosphorylation of the translation initiation factor eIF2α. Mol Cell Biol. 2002;22:7405–16.
22. Bi M, Naczki C, Koritzinsky M, Fels D, Blais J, Hu N, Harding H, Novoa I, Varia M, Raleigh J. ER stress-regulated translation increases tolerance to extreme hypoxia and promotes tumor growth. EMBO J. 2005;24:3470–81.
23. Puri P, Mirshahi F, Cheung O, Natarajan R, Maher JW, Kellum JM, Sanyal AJ. Activation and dysregulation of the unfolded protein response in nonalcoholic fatty liver disease. Gastroenterology. 2008;134:568–76.
24. Deng J, Lu PD, Zhang Y, Scheuner D, Kaufman RJ, Sonenberg N, Harding HP, Ron D. Translational repression mediates activation of nuclear factor kappa B by phosphorylated translation initiation factor 2. Mol Cell Biol. 2004;24:10161–8.
25. Jiang HY, Wek SA, McGrath BC, Scheuner D, Kaufman RJ, Cavener DR, Wek RC. Phosphorylation of the α subunit of eukaryotic initiation factor 2 is required for activation of NF-κB in response to diverse cellular stresses. Mol Cell Biol. 2003;23:5651–63.
26. Hamanaka RB, Bobrovnikova-Marjon E, Ji X, Liebhaber SA, Diehl JA. PERK-dependent regulation of IAP translation during ER stress. Oncogene. 2009;28:910–20.
27. Kazemi S, Mounir Z, Baltzis D, Raven JF, Wang S, Krishnamoorthy JL, Pluquet O, Pelletier J, Koromilas AE. A novel function of eIF2α kinases as inducers of the phosphoinositide-3 kinase signaling pathway. Mol Biol Cell. 2007;18:3635–44.
28. Mounir Z, Krishnamoorthy JL, Wang S, Papadopoulou B, Campbell S, Muller WJ, Hatzoglou M, Koromilas AE. Akt determines cell fate through inhibition of the PERK-eIF2a phosphorylation pathway. Sci Signal. 2011;4:ra62.
29. Hu P, Han Z, Couvillon AD, Exton JH. Critical role of endogenous Akt/IAPs and MEK1/ERK pathways in counteracting endoplasmic reticulum stress-induced cell death. J Biol Chem. 2004;279:49420–9.
30. Nakanishi K, Sakamoto M, Yamasaki S, Todo S, Hirohashi S. Akt phosphorylation is a risk factor for early disease recurrence and poor prognosis in hepatocellular carcinoma. Cancer. 2005;103:307–12.
31. Calvisi DF, Wang C, Ho C, Ladu S, Lee SA, Mattu S, Destefanis G, Delogu S, Zimmermann A, Ericsson J, et al. Increased lipogenesis, induced by AKT-mTORC1–RPS6 signaling, promotes development of human hepatocellular carcinoma. Gastroenterology. 2011;140:1071–83.
32. Alexia C, Bras M, Fallot G, Vadrot N, Daniel F, Lasfer M, Tamouza H, Groyer A. Pleiotropic effects of PI-3′ kinase/Akt signaling in human

hepatoma cell proliferation and drug-induced apoptosis. Ann N Y Acad Sci. 2006;1090:1–17.

33. Fu S, Yang L, Li P, Hofmann O, Dicker L, Hide W, Lin X, Watkins SM, Ivanov AR, Hotamisligil GS. Aberrant lipid metabolism disrupts calcium homeostasis causing liver endoplasmic reticulum stress in obesity. Nature. 2011;473:528–31.
34. Su Q, Tsai J, Xu E, Qiu W, Bereczki E, Santha M, Adeli K. Apolipoprotein B100 acts as a molecular link between lipid-induced endoplasmic reticulum stress and hepatic insulin resistance. Hepatology. 2009;50:77–84.
35. Donnelly KL, Smith CI, Schwarzenberg SJ, Jessurun J, Boldt MD, Parks EJ. Sources of fatty acids stored in liver and secreted via lipoproteins in patients with nonalcoholic fatty liver disease. J Clin Invest. 2005;115:1343–51.
36. York LW, Puthalapattu S, Wu GY. Nonalcoholic fatty liver disease and low-carbohydrate diets. Annu Rev Nutr. 2009;29:365–79.